Kinetics and Thermodynamics of Berberine Inclusion in Cucurbit[7]uril

Journal:	*The Journal of Physical Chemistry*
Manuscript ID:	jp-2014-00603g.R1
Manuscript Type:	Article
Date Submitted by the Author:	n/a
Complete List of Authors:	Miskolczy, Zsombor; Research Centre for Natural Sciences, Hungarian Academy of Sciences, Institute of Materials and Environmental Chemistry, Biczók, László; Research Centre for Natural Sciences, Hungarian Academy of Sciences, Institute of Materials and Environmental Chemistry

Kinetics and Thermodynamics of Berberine Inclusion in Cucurbit[7]uril

Zsombor Miskolczy, László Biczók*

Institute of Materials and Environmental Chemistry, Research Centre for Natural Sciences, Hungarian Academy of Sciences, P.O. Box 17, 1525 Budapest, Hungary

* Corresponding author. Fax: +36-1- 438-1143; E-mail: biczok.laszlo@ttk.mta.hu

Abstract

The kinetics and thermodynamics of berberine inclusion in cucurbit[7]uril was studied by stopped-flow method, fluorescence titrations and isothermal calorimetry in neat water. The about 500-fold fluorescence intensity enhancement upon encapsulation was exploited to monitor the complex formation in real-time at various temperatures. The rise of the fluorescence intensity could be fitted well by assuming a simple 1:1 binding equilibrium without any intermediate formation. For the rate constants of association and dissociation $(1.9\pm0.1)\times10^7$ $M^{-1}s^{-1}$ and (0.81 ± 0.08) s^{-1} were found at 298 K, respectively. The ingression into the cavity of CB7 had 32±2 kJ mol^{-1} activation enthalpy implying a constrictive binding, whereas 69±2 kJ mol^{-1} was obtained for the activation enthalpy of the egression. To reach the transition state substantial structural change had to occur when berberine passed through the tight carbonyl-rimmed portal of the macrocycle. An enthalpy-driven complexation took place with a slight entropy gain.

Key words: complexation dynamics, fluorescence, relaxation kinetics, macrocycle, activation energy

Introduction

The encapsulation of organic compounds in cucurbiturils (CBn), a class of cavitands comprised of glycoluril units linked by methylene groups, has received considerable attention because of its many analytical, catalytic, biological, pharmaceutical and material science applications.[1-8] To design tailor-made functional supramolecular systems, it is important to know the main factors influencing the rate of self-assembly and the response time to external stimuli.[9] The effect of guest molecular structure on the binding affinity has been extensively studied[10] but less information is available on the kinetics of inclusion.[1,11] The entry and exit processes were examined predominantly with cucurbit[6]uril (CB6) because the tight portals of this macrocycle slow down the exchange between bound and free guests often enabling the observation of the kinetics by NMR spectroscopy.[12,13] Because of the low solubility of CB6 in water all studies of the binding dynamics were carried out in the presence of large amount of salt or acid. A correlation was found between the rate of inclusion complex formation and the size of alkylammonium guests.[13] Kinetic measurements indicated that 4-methylbenzylammonium produces with CB6 not only inclusion but also exclusion complexes.[14] In the latter, the ammonium group interacts with one of the polar portals of the host and the aromatic moiety extends into the solvent. The equilibrium for the inclusion of protonated cyclohexylmethylamine in CB6 was reached only after several days, whereas the rates of ingression and egression were much faster for the unprotonated amine.[15] On the basis of systematic studies, Nau revealed the mechanistic details of the confinement in CB6.[15,16] Masson proposed that the threading of a protonated dialkylammonium moiety through CB6 has three steps. The incipiently formed complex is deprotonated, the uncharged amine slips through CB6, and finally, becomes reprotonated upon exiting from the other side of the cavity.[17] Kaifer and coworkers examined the temporal evolution of the cucurbit[7]uril (CB7) complex formation with a guest containing ferrocenylmethyl and adamantyl binding sites

linked to an ammonium moiety.[18] The encapsulation of both end groups in CB7 catalyzed the conversion from the ferrocenyl-embedded into the thermodynamically more stable adamantyl-included forms. The sliding of CB7 over an ammonium moiety was found to be energetically unfavorable. In a system comprising four components, different complexes were detected immediately after mixing the reactants, when the kinetics of inclusion controls the composition of the products, and in thermodynamic equilibrium.[19] More than 9 orders of magnitude slower egression of cyclohexane-1,4-diammonium was observed from CB6 than from CB7, while the rate constant of the complexation was 5×10^{11}-fold smaller in the former case.[19] The fast inclusion of guests in CB7 cavity is difficult to study. Bohne and coworkers used the competitive binding of Na^+ or H_3O^+ cations in their comprehensive study to decelerate the confinement of R-(+)-2-naphthyl-1-ethylammonium in CB7 into the timescale measurable by stopped-flow technique.[11]

To the best of our knowledge, only three papers provide information on the dynamics of complexation with CBn in neat water,[16,20,21] even though experiments in the absence of salt or acid give more reliable kinetic parameters. In acidic or saline solutions, the competitive binding of cations has to be taken into account, and the uncertainties in the equilibrium constant and in the rate constants for the cation interaction with CBn affect the results. Moreover, the lack of Arrhenius parameters for the association of CBn with metal cations or H_3O^+ precludes the evaluation of the temperature dependent measurements in salt and acid solutions. It is also unknown whether the number of cations coordinated to CBn changes with temperature. Ternary complex formation between cation and inclusion complex may also lead to complications. Therefore, our main objective was to systematically examine the kinetics of inclusion in CB7 in neat water and to reveal whether the encapsulation of the guest is a single step process or any intermediate can be detected. To slow down the fast bimolecular association with the host low concentration of reactants should be employed. Thus, the high

fluorescence quantum yield of the inclusion complex is a great advantage for reaching good signal to noise ratio when the binding is followed in real time. The ideal guest is practically nonfluorescent in water, but strongly emits in the cavity of CB7. We wanted to avoid the involvement of acid-base equilibrium, hence a guest without protonable or deprotonable moiety was sought. Photochemical stability and sufficient solubility in water were also essential.

Berberine (B^+), a clinically important isoquinoline alkaloid meets all these requirements. Its fluorescent behavior is very sensitive to the microenvironment.[22-24] About 500-fold fluorescence intensity enhancement was observed upon its inclusion in CB7.[25] In the present work, we exploit the favorable properties of B^+ to detect the complexation dynamics with CB7 after the fast mixing of the components with stopped-flow method. The formulas of the investigated substances are given in Scheme 1.

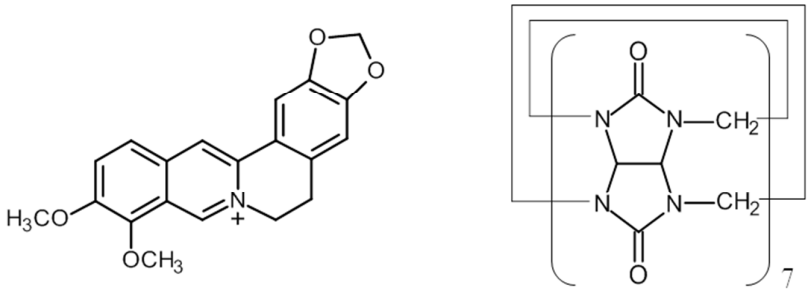

Berberine (B^+) Cucurbit[7]uril (CB7)

Scheme 1 Chemical structure of the studied compounds

Experimental Methods

Berberine chloride (Sigma) was chromatographed on silica gel (Merck) column eluting with ethanol. High purity CB7 was kindly provided by Dr Anthony I. Day (University of New South Wales, Canberra, Australia). Water was freshly distilled three times from dilute

$KMnO_4$ solution. It is important to note that spectroscopic or HPLC quality water purchased from manufacturers gave sometimes lower binding constants and slower inclusion rate due probably to the competitive binding of their trace amount of impurity. Stopped-flow measurements were performed with an Applied Photophysics RX2000 rapid mixing unit connected to a Jobin-Yvon Fluoromax-P photon-counting spectrofluorometer using a pneumatic drive. The temperature was controlled with a Julabo F25-ED thermostat. The solutions and the cuvette were kept for 15 min in the thermostated housing before mixing the reactants in 1:1 volume ratio. As initial conditions of the stopped-flow experiments, we report the concentration of the reactants immediately *after* rapid mixing. The samples were excited at 345 nm and the fluorescence intensity change was monitored at 500 nm. The slits of the monochromators corresponded to 5 nm bandpass. The time resolution was set to 5 ms/channel. At least 7 fluorescence rise profiles were averaged in the 0 – 10 s range. The data were analyzed by a home-made program written in MATLAB 7.9. Fluorescence lifetimes were determined with a previously described time-correlated single-photon counting instrument.[26]

Isothermal titration calorimetry was carried out with a VP-ITC (MicroCal) instrument at 298 K. All solutions were degassed prior to titration. B^+ solution (0.19 mM) was added stepwise in a series of 36 injections (7 μl each) from the computer-controlled microsyringe at an interval of 270 s into a 1.433 ml cell containing 0.014 mM CB7 solution, while stirring at 300 rpm. The dilution heat, which was determined by adding B^+ solution into water under the same condition as in the titration of CB7 was subtracted. The results were analyzed with the one-site binding model using Microcal ORIGIN software. The first data point was always removed. The titrations were repeated three times.

Results and Discussion

Complex formation at 283 K

B^+ has negligible emission in water,[27] but fluoresces in the 440-700 nm domain with a quantum yield of 0.23 in the nonpolar cavity of CB7.[25] Therefore, the fluorescence intensity change directly reflects the alteration of the 1:1 B^+–CB7 complex concentration. The singlet-excited B^+ is not released from the host because its lifetime in CB7 (11.6 ns)[23] is much shorter than the rate of egression. Figure 1 shows the fluorescence intensity vs. time traces at

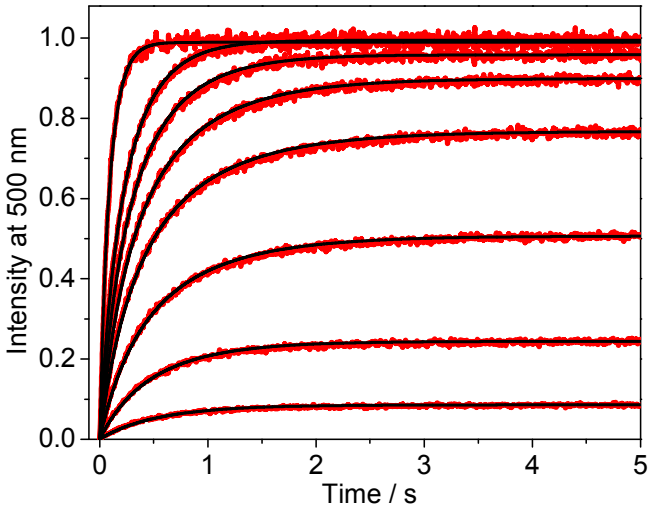

Figure 1. Alteration of the stopped-flow signals in 0.23 μM B^+ aqueous solution in the presence of 0.04, 0.07, 0.15, 0.22, 0.29, 0.40, 0.54 and 1.29 μM CB7 at 283 K. Excitation at 345 nm. The black lines represent the result of the nonlinear least-squares analysis.

various initial CB7 concentrations at 283 K. The initial B^+ concentration after rapid mixing with CB7 in a stopped-flow apparatus was kept constant (0.23 μM). The gradual increase of the host amount enhanced the initial slope of the signals due to the acceleration of the bimolecular inclusion process, and brought about a growth of the limiting value of the fluorescence intensity (I_{eq}) attained in the equilibrium. Figure 2 presents the variation of I_{eq} with the CB7 concentration. The line displays the result of the nonlinear least- squares fit of

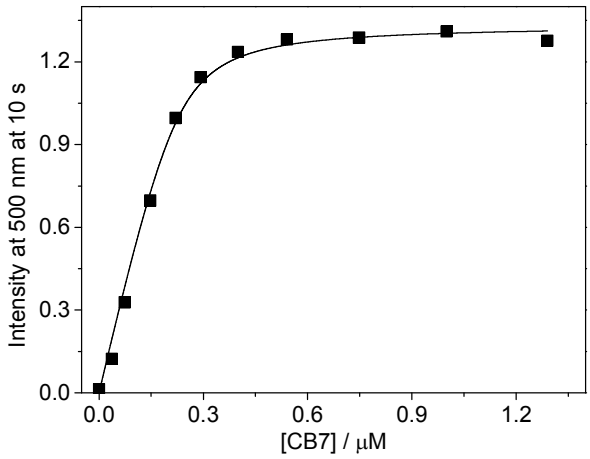

Figure 2. Fluorescence intensity at 500 nm after the attainment of the equilibrium (10 s reaction time) as a function of CB7 concentration at 283 K. $[B^+]$ = 0.23 μM

the function derived for 1:1 complexation.[28] K = (5.3±0.7)×10^7 M^{-1} was obtained for the binding constant at 283 K in agreement with the corresponding value measured by steady-state fluorescence titrations (K = (5.0±0.5)×10^7 M^{-1}).

In the case of a simple binding equilibrium, the kinetics of B^+–CB7 complex formation is defined as follows:

$$\frac{d[B-CB7]}{dt} = k_+[B^+][CB7] - k_-[B^+ - CB7] \qquad (1)$$

where k_+ and k_- denote the rate constants for complexation and dissociation. The fit of the numerical solution of the differential equation to the stopped-flow results provides k_+= (8.8±0.6)×10^6 $M^{-1}s^{-1}$ and k_-= 0.16±0.02 s^{-1}. The rate constants grow to k_+= (1.9±0.1)×10^7 $M^{-1}s^{-1}$ and k_-= 0.81±0.08 s^{-1} values at 298 K indicating the substantial temperature dependence of both the inclusion and dissociation kinetics. The k_+/k_- ratios always agree well with the corresponding binding constants determined by steady-state fluorescence titrations.

To confirm the derived rate constants, equimolar solutions of B^+ and CB7 were diluted to 0.16 μM by adding water in a stopped flow apparatus. The initial fluorescence intensity decayed due to the dissociation of the inclusion complex and a new equilibrium was reached. From the analysis of the experimental data k_+= (8.4±0.8)×10^6 $M^{-1}s^{-1}$ and k_-= 0.17±0.02 s^{-1} values were obtained at 283 K in accordance with the results acquired by mixing B^+ and CB7 solutions.

Determination of thermodynamic parameters

The fluorescence titrations of B^+ with CB7 were repeated at various temperatures (*T*) to gain insight into the factors controlling the thermodynamics of the reversible binding. From the *K* values the enthalpy (*ΔH*) and entropy change (*ΔS*) of inclusion complex formation were calculated on the basis of the relationship:

$$K = \exp(\frac{\Delta S}{R})\exp(-\frac{\Delta H}{RT}) \quad (2)$$

where *R* is the gas constant. Figure 3 displays the alteration of *K* with growing reciprocal temperature. About 32-fold diminution is observed upon warming the solution from 283 to

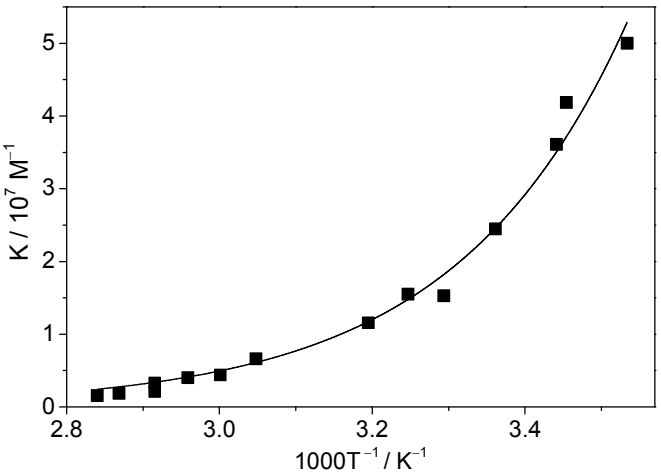

Figure 3. Equilibrium constant of B^+ confinement in CB7 as a function of reciprocal temperature. The line represents the fitted function.

352 K. The nonlinear least-squares fit of the experimental data results in ΔH = −37±2 kJ mol^{-1} and ΔS = 17±6 J mol^{-1} K^{-1} indicating that the embedment in CB7 macrocycle is an enthalpy controlled process.

To verify the derived thermodynamic parameters isothermal titration calorimetry (ITC) method was used, which directly measures the evolved reaction heat. Figure 4 shows the amount of heat produced following each injection of B^+ solution. The integrated signals, after correction with the very small dilution heat, were divided by the mole number of injectant, and the result was plotted as a function of [B^+]/[CB7] ratio in the lower panel. An inflexion point appeared around 1:1 molar ratio confirming equimolar binding stoichiometry. The analysis of the data with a one-site binding model gave K= 2.4×10^7 M^{-1}

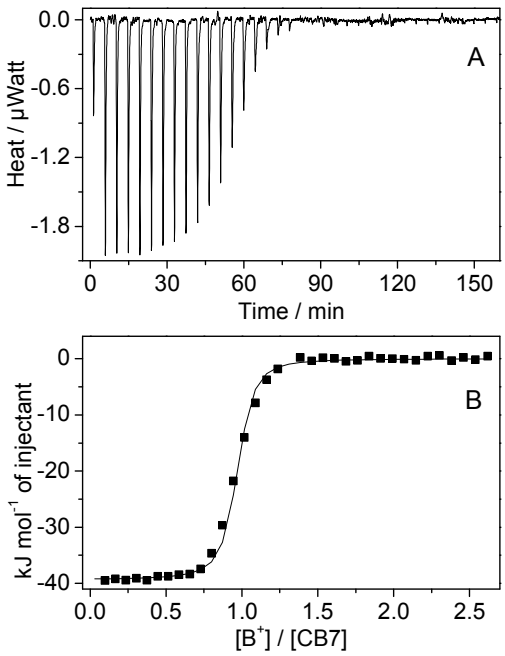

Figure 4. The results of ITC titration (A) and the integrated heat released per injection (B) (■) for the titration of 0.014 mM CB7 by 0.19 mM B^+ solution at 298 K. The line represents the best fit with a one-site binding model.

and $\Delta H = -38 \pm 2$ kJ mol^{-1}. From these quantities ΔS= 13±4 J mol^{-1} K^{-1} was calculated on the basis of the equation: $\Delta S = \Delta H/T + R \ln K$. The parameters are in fair agreement with those obtained from fluorescence titrations.

Temperature effect on the binding kinetics

To get information on the properties of the transition state of inclusion complex formation, the kinetics of B^+ interaction with CB7 was studied by stopped-flow method at various

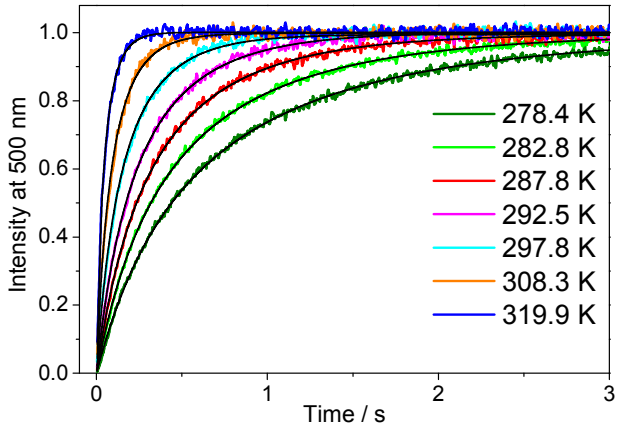

Figure 5. Rise of the fluorescence intensity in 0.23 μM B^+ and 0.23 μM CB7 aqueous solution after rapid mixing of the reactants at various temperatures. The signals were normalized at the intensity corresponding to the equilibrium. Black lines represent the calculated curves.

temperatures. The reaction rate significantly accelerated upon gradual increase of temperature. Figure 5 demonstrates that the functions calculated assuming a simple one-step binding equilibrium (vide supra) match the stopped-flow signals very well corroborating the lack of intermediate formation in the course of encapsulation. The derived rate constants (k) were fitted with the Arrhenius equation:

$$k = A \exp(-E_a/RT) \quad (3)$$

The calculated activation energies (E_a) and A-factors for the B^+ ingression into CB7 and the

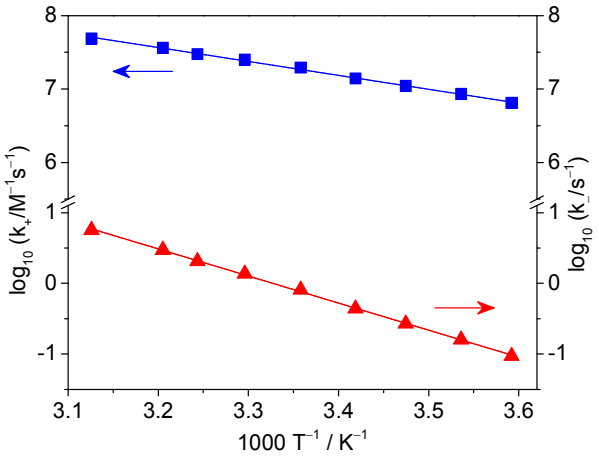

Figure 6. The logarithm of the rate constants for B^+ ingression (blue) and egression (red) vs reciprocal temperature. The lines represent the results of the nonlinear fit of the Arrhenius equation on a logarithmic scale.

Table 1. Kinetic and thermodynamic parameters for the reversible confinement of B^+ in CB7

	Ingression	Egression
E_a	35±2 kJ mol^{-1}	71±2 kJ mol^{-1}
A	(2.0±1.0)×10^{13} M^{-1}s^{-1}	(1.8±1.0)×10^{12} s^{-1}
$\Delta H^{\ddagger}$	32±2 kJ mol^{-1}	69±2 kJ mol^{-1}
$\Delta S^{\ddagger}$	2.6±1.9 J mol^{-1}K^{-1}	−19±3 J mol^{-1}K^{-1}
ΔH^{a}	− 37±2 kJ mol^{-1}	
ΔH^{b}	−38±2 kJ mol^{-1}	
ΔS^{a}	17±6 J mol^{-1}K^{-1}	
ΔS^{b}	13±4 J mol^{-1}K^{-1}	

[a] from steady-state fluorescence titrations, [b] from ITC measurements

dissociation of the inclusion complex are listed in Table 1, whereas the Arrhenius plot of the experimental and calculated data are presented in Figure 6. The *A*-factors of inclusion is about one order of magnitude larger than that of the release of B^+, whereas the activation energy has an opposite trend. The difference of the E_a values for the forward and backward reactions gives the enthalpy change in the complex formation. As expected, ΔH determined from kinetic measurements is in accordance with those obtained by ITC method and steady-state fluoresce titrations. E_a and A are empirical parameters characterizing the temperature dependence of the rate constants. Because no intermediate is found in the course of B^+–CB7 formation, the meaning of Arrhenius parameters can be rationalized on the basis of the transition state theory from which the Eyring-Polanyi equation was derived:

$$k = \kappa \frac{k_B T}{h} \exp\left(\frac{\Delta S^{\ddagger}}{R}\right) \exp\left(-\frac{\Delta H^{\ddagger}}{RT}\right) \quad (4)$$

where k_B, h, $\Delta S^{\ddagger}$, and $\Delta H^{\ddagger}$ stand for the Boltzman and Planck constants, standard entropy and enthalpy of activation, respectively. The transmission coefficient (κ) is usually taken as unity. From the comparison of eqs 3 and 4 the following relationships can be deduced:

$$E_a = \Delta H^{\ddagger} + RT \quad (5)$$

$$A = \mathrm{e} \frac{k_B T}{h} \exp\left(\frac{\Delta S^{\ddagger}}{R}\right) \quad (6)$$

The standard $\Delta H^{\ddagger}$ and $\Delta S^{\ddagger}$ values calculated using these formulas are included in Table 1.

Discussion

B^+ proved to be a particularly suitable fluorescent compound for the study of the kinetics and mechanism of the reversible inclusion in CB7. Its unique photophysical properties allowed us to monitor directly the extent of complex formation in real time with exceptionally high

sensitivity. The large fluorescence intensity change upon embedment in CB7 permitted the use of dilute solutions in which the bimolecular inclusion is sufficiently slow to follow the kinetics in neat water.

We did not observe any evidence for intermediate formation in accordance with Bohne and coworkers' results on R-(+)-2-naphthyl-1-ethylammonium confinement in CB7.[11] When CB6 served as a host, a simple equilibrium was inadequate to rationalize the binding kinetics of organic ammonium cations.[14-17] Yu and coworkers found that the dissociation of neutral guests occurs in one step from CB7, but ammonium cyclohexyl derivatives egress in multi-step processes.[29] The hydrophobic, ion–dipole and hydrogen bonding interactions are the strongest in different guest positions in CB7. The mismatch of these three interactions was suggested to cause the fast exchange between free and CB7-bound guests.[29] Nau and coworkers proposed on the basis of a comprehensive mechanistic study of the inclusion in CB6 that first an exclusion complex is produced by the coordination of the ammonium group to the negatively charged portal, and the organic moiety pivots into the cavity in a second step retaining the interaction with the macrocycle rim.[15] Such a flip-flop mechanism cannot take place with B^+ due to its bulkiness and the lack of a hydrogen bond donor site which could contribute to the stabilization of the exclusion complex. Moreover, its delocalized positive charge and hydrophobic character may render the exclusion complex formation energetically unfavorable.

NMR measurements and quantum chemical calculations have shown that the methoxy-isoquinoline moiety of B^+ is embedded in CB7, and the heterocyclic nitrogen is located in the vicinity of a carbonyl-fringed portal, whereas the benzodioxole part remains outside the macrocycle.[25] Although hydrophobic and charge-dipole host-guest interactions contribute to the stabilization of the inclusion complex, the strongly negative binding enthalpy (Table 1) may arise primarily from the removal of the high-energy water from the

hydrophobic core of the macrocycle.[30,31] CB7 contains on average 7.9 water molecules, which do not form energetically stable hydrogen bond network and their electrostatic interactions are weaker in the interior of the nonpolar, extremely nonpolarizable host than in the bulk solution.[32] The water molecules expelled by B^+ from CB7 reassemble in the bulk leading to substantial enthalpy gain. The energy needed for the desolvation of B^+ probably has only a minor effect on ΔH because of the hydrophobic character and delocalized charge of this guest.

The entropy gain in B^+–CB7 formation implies that the entropy loss originating from the host-guest association and the integration of the released water molecules into the bulk solution are overcompensated by the entropy benefit in the removal of water from the CB7 cavity and from the solvate shell of B^+. Enthalpy–entropy compensation has been observed for a wide variety of inclusion complexes because the strong interactions characterized by a large enthalpy gain usually restrict the movement of the constituents resulting in a considerable entropy loss.[33,34] The ΔS for B^+–CB7 formation is somewhat more favorable than that anticipated on the basis of the entropy–enthalpy correlation plot of CB7 complexes.[1] This probably arises from two main reasons. (i) The rigidity of the host and guest ensures that few degrees of freedom become limited by inclusion. (ii) Practically all water is liberated from CB7 by the confinement of the bulky B^+. The latter factor is corroborated by the long fluorescence lifetime of B^+ in CB7 (τ_F=11.6 ns),[25] which is close to that found in the moderately polar CH_2Cl_2 solvent (τ_F=14.3 ns).[23] The τ_F value of B^+ is highly sensitive to the interaction with water. It is about 40 ps in water[24] and 2.0 ns for 1:1 inclusion complex with cucurbit[8]uril (CB8). The much shorter τ_F in CB8 compared to CB7 proves that a significant amount of water remains in CB8 after 1:1 complex formation, but most of water molecules are expelled from CB7 upon B^+ embedment.

Due to the large size of B^+ the rate constant of its entry into CB7 was found to be significantly lower (1.9×10^7 $M^{-1}s^{-1}$ at 298 K) than that of the diffusion controlled processes in water (k_{diff} = 6.5×10^9 $M^{-1}s^{-1}$).[35] The much less voluminous 6-methoxy-N-methyl-quinolinium[21] and R-(+)-2-naphthyl-1-ethylammonium[11] cations encapsulated in CB7 with a rate constant (k_+) of 3.0×10^9 and 6.3×10^8 $M^{-1}s^{-1}$, respectively. The more rapid processes for the latter two compounds suggest that the size of the guest relative to the opening of the CB7 macrocycle is an important factor controlling the rate of association. Interestingly, the ingression of ethyl benzyl ketone to CB7 occurs even slower[20] ($k_+ = 4.6\times10^6$ $M^{-1}s^{-1}$) than B^+ inclusion. This may indicate that the activation enthalpy or the activation entropy is less favorable for the confinement of an uncharged guest. The k_+ values for the binding to CB7 are several orders of magnitude larger than the corresponding rate constants for the complexation with CB6,[12,13,16] which typically fall in the range of 0.4 – 6000 $M^{-1}s^{-1}$. The slower inclusion in the smaller cavitands homologue is only partly due to the competitive binding of cations or acids, which are used to dissolve CB6. In the case of cyclohexylammonium association with CB6, the effect of salt amount was studied, and k_+ = 0.44 $M^{-1}s^{-1}$ can be derived from the reported data for 0 M salt concentration.[16]

The rate constant of B^+–CB7 dissociation is almost two orders of magnitude smaller than k_- for R-(+)-2-naphthyl-1-ethylammonium[11] (55 s^{-1}), while more than 1000-fold slower than the egression of ethyl benzyl ketone[20] (10^3 s^{-1}) and 6-methoxy-N-methylquinolinium[21] (1.5×10^3 s^{-1}). The substantial alteration of k_- with the molecular structure of the guests presumably attributable mainly to the change of the activation energy of inclusion complex dissociation, but Arrhenius parameters have not been published previously for the reversible binding to CB7.

We found large activation enthalpy for B^+–CB7 complex formation (Table 1) suggesting that a substantial steric barrier must be overcome in the course of inclusion. This is in a sharp contrast with the binding in 4-sulfonatocalixarenes, whose macrocycle allows unobstructed insertion of B^+.[22] Kinetically controlled inclusion complex stability was observed for hemicarceplexes, whose formation is characterized by much larger activation energy than the free energy gain in the reaction.[36] Cram introduced the concept of constrictive binding for the phenomenon when the entry into and exit from a relatively rigid cavitand is sterically inhibited, and the guest is entrapped because of the large activation energy of the exchange process.[37,38] Unlike hemicarceplexes, B^+ is only partially embedded in CB7 and the activation enthalpy of association is comparable to the enthalpy gain in the association. X-ray crystallographic measurements showed[39] that the openings of CB7 has a diameter of 0.54 nm, but the equatorial internal width is significantly larger, 0.73 nm. Hence, B^+ can be accommodated in this host after squeezing through the tight carbonyl-laced portal. An oval distortion of the opening may promote the access of the interior. The enhanced conformational motions in the reactants at elevated temperature facilitate the attainment of the molecular geometry of the transition state. A large ellipsoidal deformation of CB6 skeleton was reported to takes place even in the ground state when p-xylylenediammonium or phenylenediammonium cations were embedded.[40,41] Nau and coworkers inferred from the marked decrease of the ingression rate with increasing steric demand of the guest that constrictive binding also applies for CB6.[15,16]

The close to zero activation entropy of B^+ ingression into CB7 implies that the entropy penalty paid upon the ordering of the reactants into the transition state is offset by the entropy gain upon partial desolvation. The reverse process has a negative activation entropy suggesting that the entropy growth arising from the looser binding in the transition state

compared to the inclusion complex only partially compensates the substantial entropy loss originating from the coordination of water.

The slow escape of B^+ from CB7 is attributed to the sizable (69 kJ mol^{-1}) activation enthalpy. Both the binding enthalpy (ΔH) and the activation enthalpy of ingression must be supplied to reach the transition state of B^+ egression. The former component (ΔH) has about 5 kJ mol^{-1} larger contribution to the enthalpy barrier, which must be overcome when B^+ exits from CB7, compared to the activation enthalpy of ingression.

Conclusions

The direct detection of the encapsulation and exit kinetics in neat water provided evidences for the single-step reversible binding of B^+ in CB7 without formation of any intermediate in the longer than 10 ms time scale. The rate constant was found to be about 400-fold slower for the ingression into the nonpolar cavity of CB7 than for a diffusion controlled process because the tight portal of the host led to a constrictive binding. The large activation enthalpy of B^+ egression from CB7 caused the slow dissociation and the high stability of the inclusion complex. The substantial enthalpy gain upon B^+ confinement was due primarily to the release of high energy water from the CB7 interior. The long fluorescence lifetime of the encapsulated B^+ indicated that most of the water molecules were expelled from the macrocycle in the course of inclusion complex formation. The in-depth understanding of the various factors controlling the thermodynamics and kinetics of host-guest binding in CB7 facilitates the rational design of tailor-made self-sorting systems, controlled release formulations, molecular switches and molecular machines. To tune the operational speed of CB7 complexes in these applications, the knowledge of the correlation between molecular structure and the kinetics of reversible complexation is required. The utilization of B^+ as a

fluorescent probe may open up new possibilities for the study of the kinetics of competitive binding of various guests.

Acknowledgement

The authors very much appreciate the support of this work by the Hungarian Scientific Research Fund (OTKA, Grant K104201). This paper was supported by the János Bolyai Research Scholarship of the Hungarian Academy of Sciences.

References

(1) Masson, E.; Ling, X.; Joseph, R.; Kyeremeh-Mensah, L.; Lu, X. Cucurbituril Chemistry: A Tale of Supramolecular Success. *RSC Advances* **2012**, *2*, 1213-1247.

(2) Walker, S.; Oun, R.; McInnes, F. J.; Wheate, N. J. The Potential of Cucurbit[n]urils in Drug Delivery. *Isr. J. Chem.* **2011**, *51*, 616-624.

(3) Park, K. M.; Yang, J. A.; Jung, H.; Yeom, J.; Park, J. S.; Park, K. H.; Hoffman, A. S.; Hahn, S. K.; Kim, K. In Situ Supramolecular Assembly and Modular Modification of Hyaluronic Acid Hydrogels for 3d Cellular Engineering. *ACS Nano* **2012**, *6*, 2960-2968.

(4) Ghosh, I.; Nau, W. M. The Strategic Use of Supramolecular pK_a Shifts to Enhance the Bioavailability of Drugs. *Adv. Drug Deliv. Rev.* **2012**, *64*, 764-783.

(5) Hennig, A.; Bakirci, H.; Nau, W. M. Label-Free Continuous Enzyme Assays with Macrocycle-Fluorescent Dye Complexes. *Nature Methods* **2007**, *4*, 629-632.

(6) Pemberton, B. C.; Raghunathan, R.; Volla, S.; Sivaguru, J. From Containers to Catalysts: Supramolecular Catalysis within Cucurbiturils. *Chem. Eur. J.* **2012**, *18*, 12178-12190.

(7) Lagona, J.; Mukhopadhyay, P.; Chakrabarti, S.; Isaacs, L. The Cucurbit[n]uril Family. *Angew. Chem. Int. Ed.* **2005**, *44*, 4844-4870.

(8) Miskolczy, Z.; Biczók, L. Photochromism in Cucurbit[8]uril Cavity: Inhibition of Hydrolysis and Modification of the Rate of Merocyanine-Spiropyran Transformations. *J. Phys. Chem. B* **2011**, *115*, 12577-12583.

(9) Wook Lee, J.; Kim, K.; Kim, K. A Kinetically Controlled Molecular Switch Based on Bistable [2]Rotaxane. *Chem. Commun.* **2001**, 1042-1043.

(10) Dsouza, R. N.; Pischel, U.; Nau, W. M. Fluorescent Dyes and Their Supramolecular Host/Guest Complexes with Macrocycles in Aqueous Solution. *Chem. Rev.* **2011**, *111*, 7941-7980.

(11) Tang, H.; Fuentealba, D.; Ko, Y. H.; Selvapalam, N.; Kim, K.; Bohne, C. Guest Binding Dynamics with Cucurbit[7]uril in the Presence of Cations. *J. Am. Chem. Soc.* **2011**, *133*, 20623-20633.

(12) Mock, W. L.; Shih, N. Y. Structure and Selectivity in Host-Guest Complexes of Cucurbituril. *J. Org. Chem.* **1986**, *51*, 4440-4446.

(13) Mock, W. L.; Shih, N. Y. Dynamics of Molecular Recognition Involving Cucurbituril. *J. Am. Chem. Soc.* **1989**, *111*, 2697-2699.

(14) Hoffmann, R.; Knoche, W.; Fenn, C.; Buschmann, H.-J. Host-Guest Complexes of Cucurbituril with the 4-Methylbenzylammonium Ion, Alkali-Metal Cations and NH_4^+. *J. Chem. Soc., Faraday Trans.* **1994**, *90*, 1507-1511.

(15) Marquez, C.; Nau, W. M. Two Mechanisms of Slow Host–Guest Complexation between Cucurbit[6]uril and Cyclohexylmethylamine: pH-Responsive Supramolecular Kinetics. *Angew. Chem. Int. Ed.* **2001**, *40*, 3155-3160.

(16) Márquez, C.; Hudgins, R. R.; Nau, W. M. Mechanism of Host−Guest Complexation by Cucurbituril. *J. Am. Chem. Soc.* **2004**, *126*, 5806-5816.

(17) Ling, X.; Samuel, E. L.; Patchell, D. L.; Masson, E. Cucurbituril Slippage: Translation Is a Complex Motion. *Org. Lett.* **2010**, *12*, 2730-2733.

(18) Tootoonchi, M. H.; Yi, S.; Kaifer, A. E. Detection of Isomeric Microscopic Host–Guest Complexes. A Time-Evolving Cucurbit[7]uril Complex. *J. Am. Chem. Soc.* **2013**, *135*, 10804-10809.

(19) Mukhopadhyay, P.; Zavalij, P. Y.; Isaacs, L. High Fidelity Kinetic Self-Sorting in Multi-Component Systems Based on Guests with Multiple Binding Epitopes. *J. Am. Chem. Soc.* **2006**, *128*, 14093-14102.

(20) Mezzina, E.; Cruciani, F.; Pedulli, G. F.; Lucarini, M. Nitroxide Radicals as Probes for Exploring the Binding Properties of the Cucurbit[7]uril Host. *Chem. Eur. J.* **2007**, *13*, 7223-7233.

(21) Miskolczy, Z.; Harangozo, J. G.; Biczok, L.; Wintgens, V.; Lorthioir, C.; Amiel, C. Effect of Torsional Isomerization and Inclusion Complex Formation with Cucurbit[7]uril on the Fluorescence of 6-Methoxy-1-Methylquinolinium. *Photochem. Photobiol. Sci.* **2014**, *13*, DOI: 10.1039/C1033PP50307K.

(22) Megyesi, M.; Biczók, L. Considerable Fluorescence Enhancement upon Supramolecular Complex Formation between Berberine and *p*-Sulfonated Calixarenes. *Chem. Phys. Lett.* **2006**, *424*, 71-76.

(23) Megyesi, M.; Biczók, L. Effect of Ion Pairing on the Fluorescence of Berberine, a Natural Isoquinoline Alkaloid. *Chem. Phys. Lett.* **2007**, *447*, 247-251.

(24) Megyesi, M.; Biczók, L. Berberine Alkaloid as a Sensitive Fluorescent Probe for Bile Salt Aggregates. *J. Phys. Chem. B* **2007**, *111*, 5635-5639.

(25) Megyesi, M.; Biczók, L.; Jablonkai, I. Highly Sensitive Fluorescence Response to Inclusion Complex Formation of Berberine Alkaloid with Cucurbit[7]uril. *J. Phys. Chem. C* **2008**, *112*, 3410-3416.

(26) Megyesi, M.; Biczók, L. Considerable Change of Fluorescence Properties upon Multiple Binding of Coralyne to 4-Sulfonatocalixarenes. *J. Phys. Chem. B* **2010**, *114*, 2814-2819.

(27) Inbaraj, J. J.; Kukielczak, B. M.; Bilski, P.; Sandvik, S. L.; Chignell, C. F. Photochemistry and Photocytotoxicity of Alkaloids from Goldenseal (Hydrastis Canadensis L.) 1. Berberine. *Chem. Res. Toxicol.* **2001**, *14*, 1529-1534.

(28) Valeur, B. *Molecular Fluorescence, Principles and Applications*; Wiley-VCH: Weinheim, 2002.

(29) Yu, J. S.; Wu, F. G.; Tao, L. F.; Luo, J. J.; Yu, Z. W. Mechanism of the Fast Exchange between Bound and Free Guests in Cucurbit[7]uril-Guest Systems. *Phys. Chem. Chem. Phys.* **2011**, *13*, 3638-3641.

(30) Nau, W. M.; Florea, M.; Assaf, K. I. Deep inside Cucurbiturils: Physical Properties and Volumes of Their Inner Cavity Determine the Hydrophobic Driving Force for Host–Guest Complexation. *Isr. J. Chem.* **2011**, *51*, 559-577.

(31) Biedermann, F.; Vendruscolo, M.; Scherman, O. A.; De Simone, A.; Nau, W. M. Cucurbit[8]uril and Blue-Box: High-Energy Water Release Overwhelms Electrostatic Interactions. *J. Am. Chem. Soc.* **2013**, *135*, 14879-14888.

(32) Biedermann, F.; Uzunova, V. D.; Scherman, O. A.; Nau, W. M.; De Simone, A. Release of High-Energy Water as an Essential Driving Force for the High-Affinity Binding of Cucurbit[n]urils. *J. Am. Chem. Soc.* **2012**, *134*, 15318-15323.

(33) Liu, L.; Guo, Q. X. Isokinetic Relationship, Isoequilibrium Relationship, and Enthalpy-Entropy Compensation. *Chem. Rev.* **2001**, *101*, 673-695.

(34) Rekharsky, M. V.; Inoue, Y. Complexation Thermodynamics of Cyclodextrins. *Chem. Rev.* **1998**, *98*, 1875-1917.

(35) Montalti, M.; Credi, A.; Prodi, L.; Gandolfi, M. T. *Handbook of Photochemistry; 3rd Ed.*; CRC Press: Boca Raton, FL: Boca Raton, FL,, 2006.

(36) Cram, D. J.; Blanda, M. T.; Paek, K.; Knobler, C. B. Constrictive and Intrinsic Binding in a Hemicarcerand Containing Four Portals. *J. Am. Chem. Soc.* **1992**, *114*, 7765-7773.

(37) Quan, M. L. C.; Cram, D. J. Constrictive Binding of Large Guests by a Hemicarcerand Containing Four Portals. *J. Am. Chem. Soc.* **1991**, *113*, 2754-2755.

(38) Cram, D. J.; Tanner, M. E.; Knobler, C. B. Host-Guest Complexation. 58. Guest Release and Capture by Hemicarcerands Introduces the Phenomenon of Constrictive Binding. *J. Am. Chem. Soc.* **1991**, *113*, 7717-7727.

(39) Kim, J.; Jung, I.-S.; Kim, S.-Y.; Lee, E.; Kang, J.-K.; Sakamoto, S.; Yamaguchi, K.; Kim, K. New Cucurbituril Homologues: Syntheses, Isolation, Characterization, and X-Ray Crystal Structures of Cucurbit[n]uril (N = 5, 7, and 8). *J. Am. Chem. Soc.* **2000**, *122*, 540-541.

(40) Huang, W.-H.; Zavalij, P. Y.; Isaacs, L. Cucurbit[6]uril *p*-Xylylenediammonium Diiodide Decahydrate Inclusion Complex. *Acta Crystallographica Section E* **2008**, *64*, o1321-o1322.

(41) Huang, W.-H.; Zavalij, P. Y.; Isaacs, L. Cucurbit[6]uril *p*-Phenylenediammonium Diiodide Decahydrate Inclusion Complex. *Acta Crystallographica Section E* **2007**, *63*, o1060-o1062.

Table of Contents Graphics